

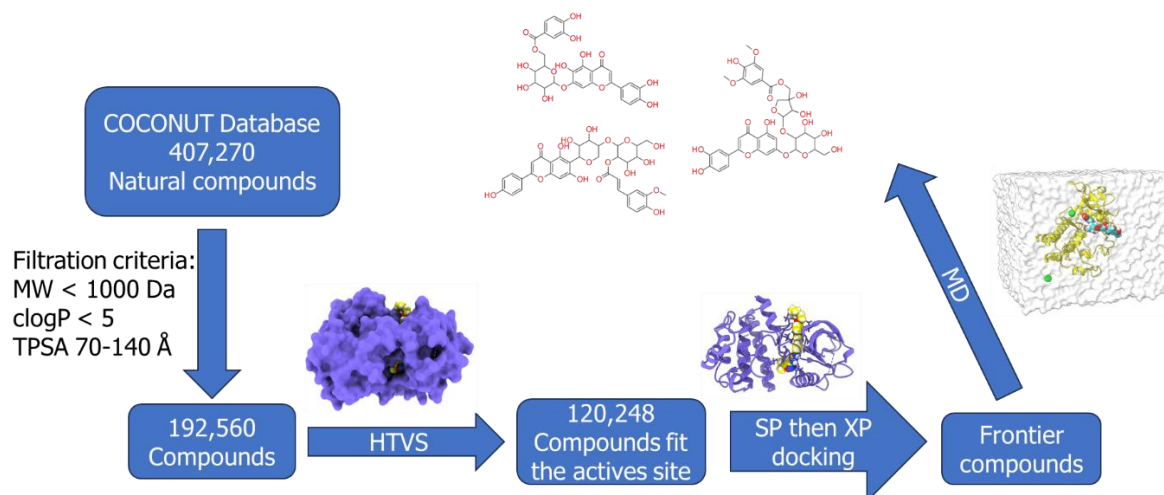
# SciRad SCIENTIAE RADICES

## Natural Products as Potential Inhibitors of FLT3 for Acute Myeloid Leukemia: HTVS, Docking, and Molecular Dynamic Simulation

Salsabeel Salah<sup>(1)</sup>, Najat Sami, Sarah Ali<sup>(1)</sup>, Teemah-Alrahman Khalid<sup>(1)</sup>, and Radwan Alnajjar<sup>(1),(2)</sup> ✉

<sup>(1)</sup> PharmD, Faculty of Pharmacy, Libyan International Medical University, Benghazi, Libya; <sup>(2)</sup> Department of Chemistry, Faculty of Science, University of Benghazi, Benghazi, Libya

✉ Correspondence to: Radwan.alnajjar@limu.edu.ly



**Abstract:** Cancer is one the most common health issues worldwide, with cancer-related mortality of 9.5 million in 2018, with an expectation to become 29.5 by 2040. Among others, acute myeloid leukemia (AML) is common among older people. FLT3 mutations are one of the most common genetic aberrations found in Acute Myeloid Leukemia and are associated with poor prognosis. Herein, we attempt to identify natural compounds as potential candidates to treat AML by targeting the FLT3 kinase domain using in silico approaches. The COCONUT database, which contains 407,270 natural compounds, was HTVS against the FLT3 kinase domain active site, and promising compounds were subject to molecular docking. Finally, frontier compounds were validated further using molecular dynamic simulation. In total, ten compounds were

identified with docking scores higher than Quizartinib (-11.606 kcal/mol), with the best three compounds showing a docking score of -18.052, -15.772, and -16.767 kcal, respectively, and compound 2 showing excellent stability in molecular dynamic simulation.

**Keywords:** Acute Myeloid Leukemia, Drug Design, Anticancer, CADD, FLT3.

**Received:** 2023.11.15

**Accepted:** 2023.11.30

**Published:** 2023.12.02

DOI: 10.58332/scirad2023v2i4a03

## Introduction

Acute Myeloid Leukemia (AML) is a hematological malignancy that is characterized by a rapid clonal expansion of abnormally differentiated myeloid progenitor cells.[1] AML is the second most common form of leukemia in adults and children, and it accounts for 31% of all adult leukemia cases.[2] The 5-year relative survival rate for people over 20 is 28%, and 69% for people younger than 20. [2] The American Cancer Society estimates that acute myeloid leukemia stats in the United States for 2023 will be 20,380 new cases and 11,310 deaths, and most of them will be adults. [2] The large majority of AML cases (about 97%) are due to genetic mutations, with the remaining cases due to inhibition of maturation of myeloid stem cells due to mutations, chromosomal translocations, or changes in molecular levels in patients with an underlying hematological disorder.[3] It is important to delineate these genetic abnormalities in order to risk stratify patients and determine appropriate treatment.[3] FMS (Feline McDonough Sarcoma)-Like Tyrosine Kinase 3 (FLT3) is a type III receptor tyrosine kinase that plays an important role in hematopoietic cell survival, proliferation, and differentiation.[4] Mutation of FLT3 is one of the most common genetic mutations, arising in 25-30% of all acute myeloid leukemia (AML) patients.[5][6] FLT3 gene mutations could be classified into two types: Internal Tandem Duplications (ITD) and Tyrosine Kinase Domains (TKD); these mutations will activate FLT3 signaling and promote blast proliferation.[5] Patients with FLT3-ITD mutations have a higher risk of relapse, which increases its clinical significance.[5] In preclinical studies, FLT3 inhibitors were capable of competing with ATP to bind to the active pocket of the kinase domain, inhibiting autophosphorylation and phosphorylation of downstream targets.[1] The first-generation FLT3 inhibitors are multi-kinase inhibitors that are not selective to FLT3, such as Midostaurin (Figure 1, 1) and Sunitinib (Figure 1, 2),[1] while second-generation FLT3 inhibitors, such as Quizartinib (Figure 1, 3) and Gilteritinib (Figure 1, 4) were developed to inhibit FLT3 mutation in patients with AML selectively.[1] Although patients initially respond very well to FLT3 inhibitors, the clinical

duration of response is often short-lived as patients relapse with more aggressive and drug-resistant diseases.[1]

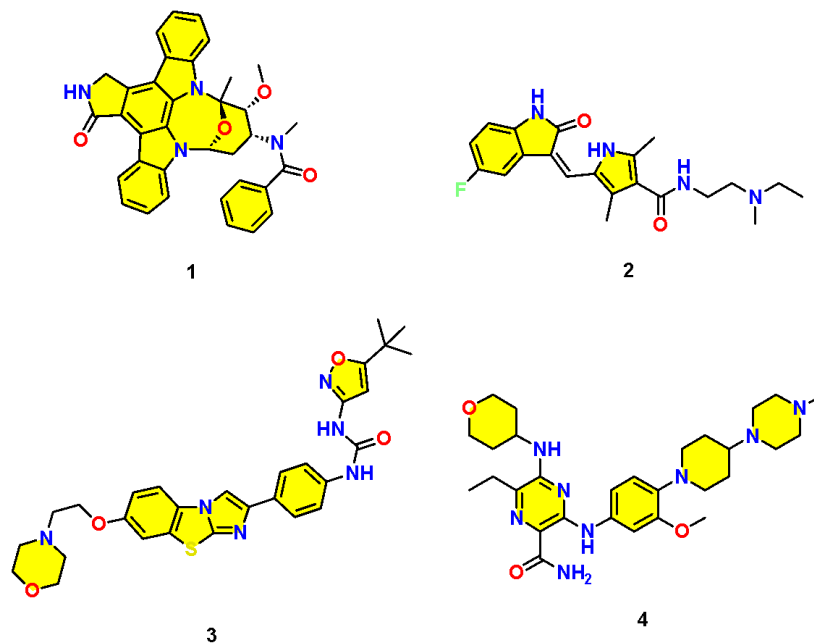


Figure 1: FLT3 Inhibitors in clinical trials

According to Yamaura et al., FF-10101 (Figure 2, 5) was confirmed to have excellent potent anti-leukemia activity in AML cells with numerous FLT3 mutations in vitro and patient-derived xenograft (PDX) models. [7] Regardless of the allelic ratio of FLT3-ITD to wild-type FLT3, FF-10101 was capable of reducing cell viability. [7]

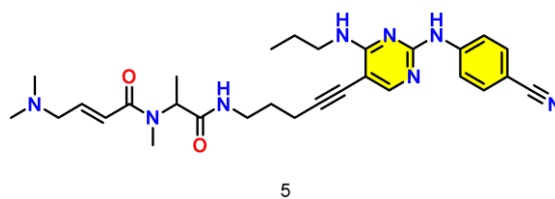
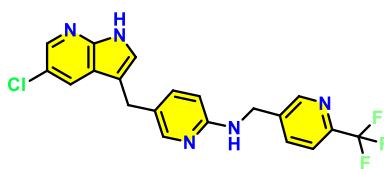


Figure 2: Chemical structure of compound FF-10101

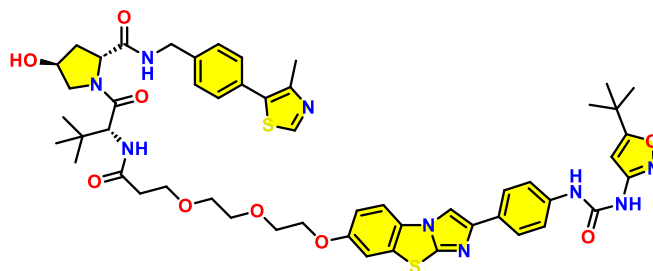
Moreover, Wang et al. reported on the development of resistance to FLT3 inhibitors and identified a triple-kinase inhibitor Pexidartinib (PLX3397) (Figure 3, 6) capable of addressing this resistance by effective strategies, such as avoiding steric hindrance with mutated residues in FLT3 receptors and introducing shorter (methyl amine) linker between the middle and tail pyridine rings that produce favorable interactions to enhance its efficacy. [8]



6

Figure 3: Chemical structure of Pexidartinib (PLX3397)

Tong et al. mentioned the ability of proteolysis targeting chimeras (PROTACs) (Figure 4, 7) to target degradation of tyrosine kinase receptors at low nanomolar concentrations that aims to develop a FLT3 PROTAC, which proved to be successful in inducing degradation of FLT3-ITD protein in MOLM-14 cells and MV4-11 cells. In comparison to quizartinib, this FLT3 PROTAC exhibited greater selectivity and more than 3.5-fold increased potency in MV4-11 cells and MOLM-14 cells. [9]



7

Figure 4: Chemical structure of PROTACs

In the past decades, incredible efforts have been made to collect novel natural products from microbes, plants, and other living organisms, to estimate their anticancer properties, and to investigate their mechanism of action.[10] It is estimated that between 1981 and 2019, approximately 25% of all newly approved anticancer drugs were derived from natural products. such as, vincristine, etoposide and paclitaxel.[10]

The purpose of this study is to find potential candidates for treating acute myeloid leukemia by targeting the FLT3 kinase domain using an available natural products database. High throughput virtual screening (HTVS) was performed on over 407,270 natural products from the COCONUT database, followed by docking and molecular dynamics. The hits underwent further pharmacokinetic studies using SwissADME to find the best ten candidate compounds as potential inhibitors.

## Results and discussion

### Molecular Docking

HTVS was conducted on the 71,230 compounds that met the criteria of filtration, followed by standard precision docking (SP) for the top 100 compounds into the active site of the FLT3 kinase domain; the top ten compounds that were obtained in the docking step are presented in Table 1.

Table 1: Docking scores of frontier candidate compounds and their interactions

Compound ID	Docking score (kcal/mol)	Residue/Interaction	Distance (Å)
1	-18.052	Asp829/HB-Acceptor	2.040
		Asp829/HB-Acceptor	1.940
		Asn701/HB-Donor	2.230
		Asp698/HB-Acceptor	2.170
		Cys694/HB-Donor	2.100
		Cys694/HB-Acceptor	1.890
2	-17.884	Arg834/HB-Donor	2.260
		Asp829/HB-Acceptor	2.170
		Asp829/HB-Acceptor	2.040
		Leu616/HB-Acceptor	1.890
		Leu616/HB-Acceptor	1.770
		Cys694/HB-Donor	1.770
		Ser618/HB-Acceptor	2.260
3	-16.767	Arg834/HB-Donor	2.220
		Asp829/HB-Acceptor	2.290
		Leu616/HB-Acceptor	1.690
		Cys694/HB-Donor	1.840
		Cys694/HB-Acceptor	1.720
		Tyr696/HB-Acceptor	1.880
4	-16.470	Asp696/HB-Acceptor	2.160
		Asp696/HB-Acceptor	1.640
		Asp696/HB-Acceptor	1.630
		Asn701/HB-Donor	1.850
		Cys694/HB-Acceptor	1.680
		Cys694/HB-Donor	2.440
5	-16.326	Cys694/HB-Acceptor	1.680
		Cys694/HB-Donor	2.440
		Asp696/HB-Acceptor	1.540
		Asp696/HB-Acceptor	1.840
		Asp696/HB-Acceptor	1.610
		Asp696/HB-Donor	1.910
		Cys694/HB-Donor	2.060
Asp829/HB-Acceptor	2.020		

		Asn701/HB-Donor	1.710
		Leu616/HB-Acceptor	1.860
6	-16.310	Asn701/HB-Donor	2.370
		Asn701/HB-Donor	2.210
		Asp698/HB-Acceptor	1.970
		Asp829/HB-Acceptor	2.350
		Cys694/HB-Donor	1.960
		Cys694/HB-Acceptor	1.630
7	-16.156	Cys694/HB-Donor	1.970
		Asp829HB-Acceptor	2.000
		Ser705/HB-Acceptor	1.690
		Cys694/HB-Donor	1.980
8	-16.055	Cys694/HB-Acceptor	2.020
		Asn626/HB-Donor	2.350
		Leu616/HB-Acceptor	2.050
		Ser705/HB-Acceptor	2.130
		Leu616/HB-Acceptor	1.980
9	-15.966	Leu616/HB-Acceptor	1.740
		Glu661/HB-Acceptor	2.000
		Cys694/HB-Acceptor	1.950
		Arg834/HB-Donor	2.310
		Cys694/HB-Donor	1.700
10	-15.772	Ser705/HB-Acceptor	1.660
		Asp698/HB-Acceptor	1.960
		Asp829/HB-Acceptor	1.630
		Asn701/HB-Donor	2.190
		Glu661/HB-Acceptor	1.890
		Cys644/HB-Donor	1.740
Quizartinib	-11.616	Cys695/HB-Acceptor	2.080
		Glu661/HB-Acceptor	2.040

The active site of the FLT3 kinase domain (PDB ID: 4XUF) has a cave shape and contains the following amino acids: His809, which is positively charged; Asp829 and Glu661, which are negatively charged. Ala612, Leu802, Leu668, Leu818, Leu616, Val624, Val675, Tyr696, Met664, Phe691, Met665, Ile827, Val675 and Tyr693 are amino acids with hydrophobic side chains, and Cys694, Cys695, Cys828 form sulfhydryl bridges, as well as Gly697. The crystal structure of the FLT3 kinase domain is presented in Figure 3.

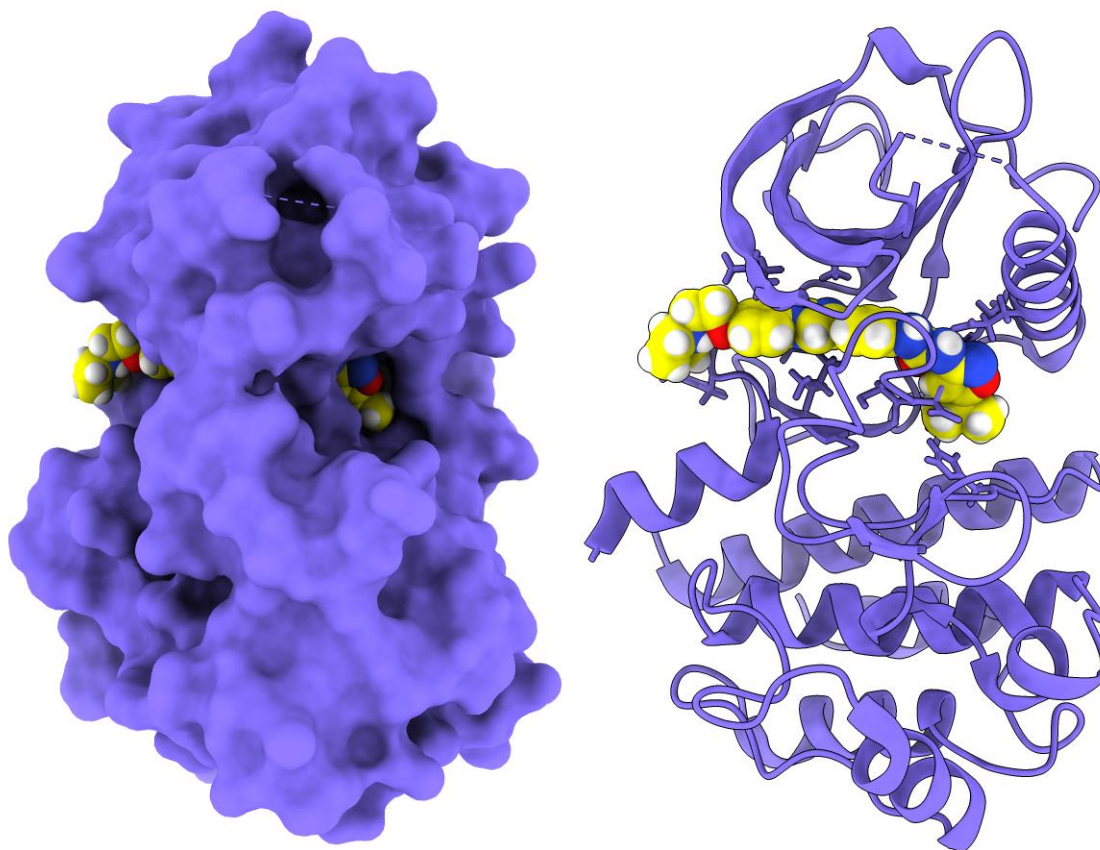


Figure 5: The crystal structure of the FLT3 kinase domain surface presentation (left) and ribbon presentation (right)

As can be seen in Table 1, compound 1 was able to form up to six hydrogen bonds (H-bond with a distance less than 3.30 Å considered strong) [11] with residues, Asp829 (2 HB), Asn701, Asp698, and Cys694 (2 HB) which results in a docking score of -18.052 kcal/mol, which indicated solid interactions with the active site of the protein. Following, compound 2 also showed an excellent docking score of -17.884 kcal/mol, and it was able to form seven H-Bonds with residues Arg834, Asp829 (2 HB), Leu616(2 HB), Cys694, and Ser618. It is worth mentioning that even though compound 2 was able to form more hydrogen bonds than compound 1, compound 1 was able to fit tight inside the cavity of the proteins and hence formed more favorable Van der Waal interactions, Figure 6.

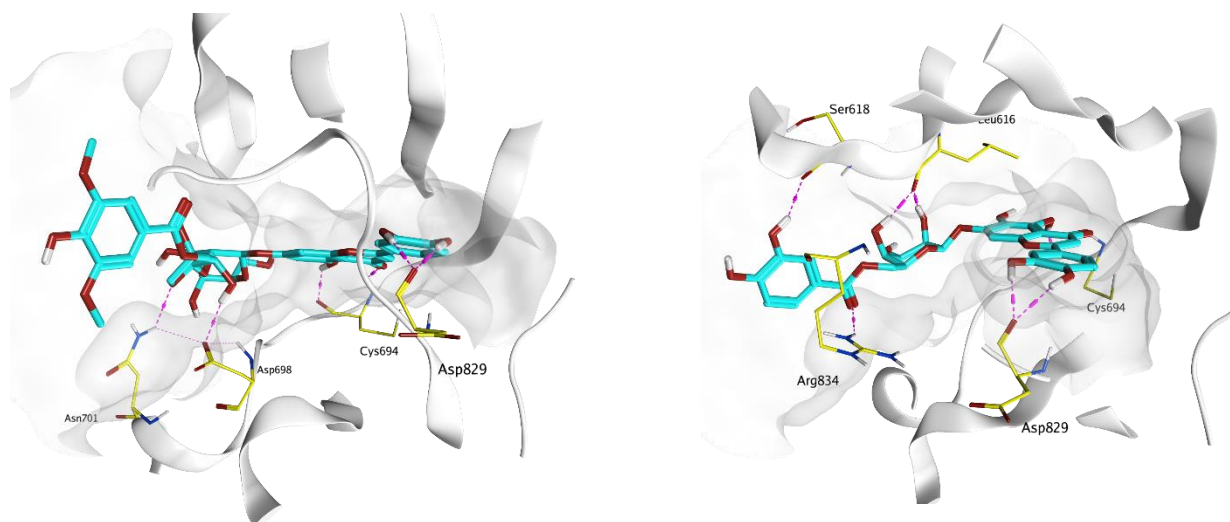


Figure 6: Interactions of compounds 1 and 2 inside the active site of the FLT3 kinase domain

Compound 3, with a docking score of -16.767 kcal/mol, and compound 4, with a docking score of -16.470 kcal/mol, were both able to form six H-bonds with protein residues.

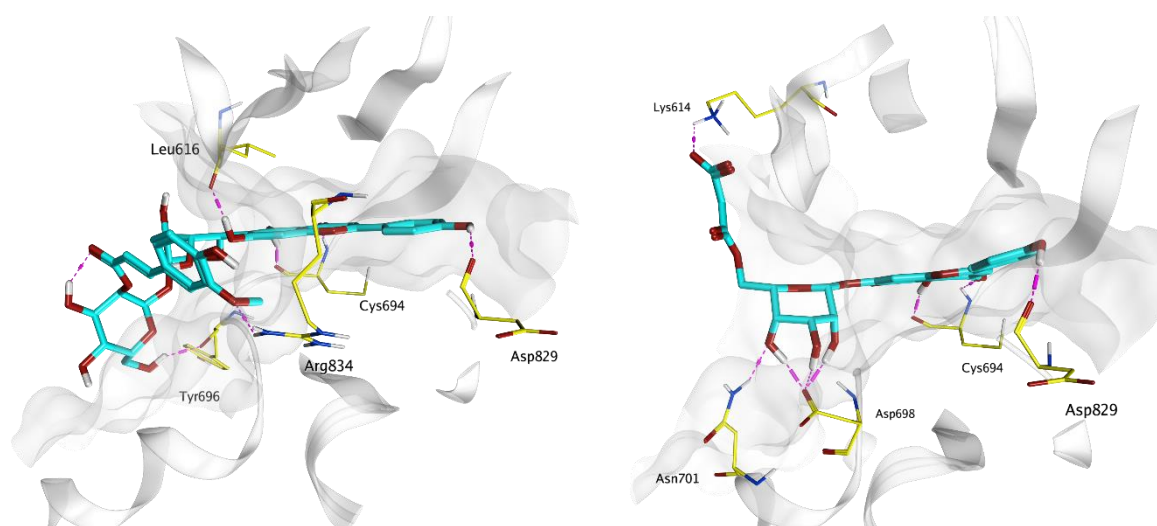


Figure 7: Interactions of compounds 3 and 4 inside the active site of the FLT3 kinase domain

Compound **5** with docking score (-16.326 kcal/mol), formed up to six H-bond with residues Cys694 (1.680 Å—Acceptor), Asp698 (1.540 Å—Acceptor, 1.840 Å—Acceptor, and 1.610 Å—Acceptor), Asp829 (2.020 Å), Asn701 (1.710 Å). Compound **6** with docking score (-16.310 kcal/mol), formed six H-bond with residues Leu616 (1.860 Å), Asn701(2.370 Å—Donor and Donor 2.210 Å—Donor), Asp698 (1.970 Å), Asp829 (2.350 Å), Cys694 (1.960 Å).



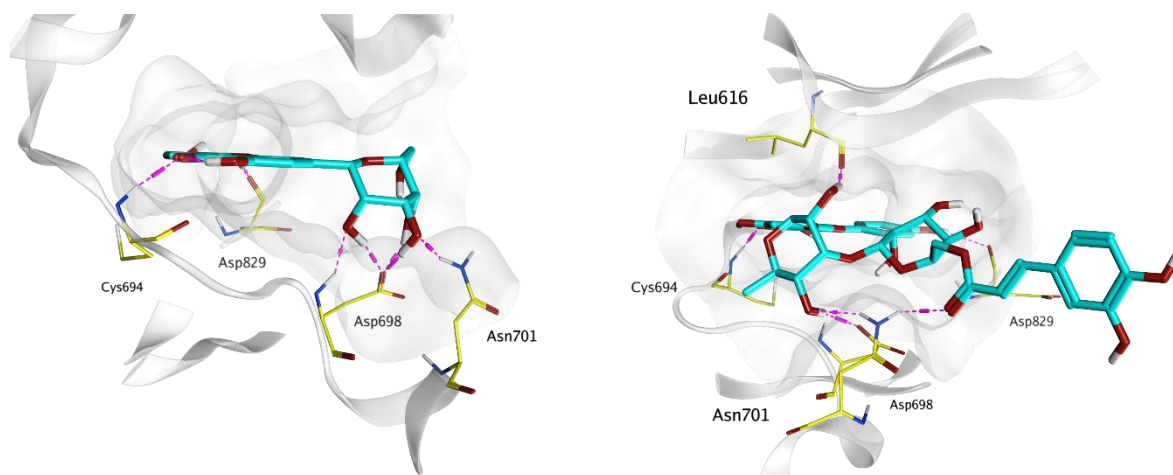


Figure 8: Interactions of compounds 5 and 6 inside the active site of the FLT3 kinase domain

Compound 7 with docking score (-16.156 kcal/mol) formed four H-bond with residues Cys694 (1.630 Å—Acceptor and 1.970 Å—Donor), Asp829 (2.0 Å), Ser705 (1.690 Å). Compound 8 with docking score (-16.055 kcal/mol) formed five H-bond with residues Cys694 (1.980 Å—Donor and 2.020 Å—Acceptor), Asn626 (2.350 Å), Leu616 (2.050 Å), Ser705 (2.130 Å).

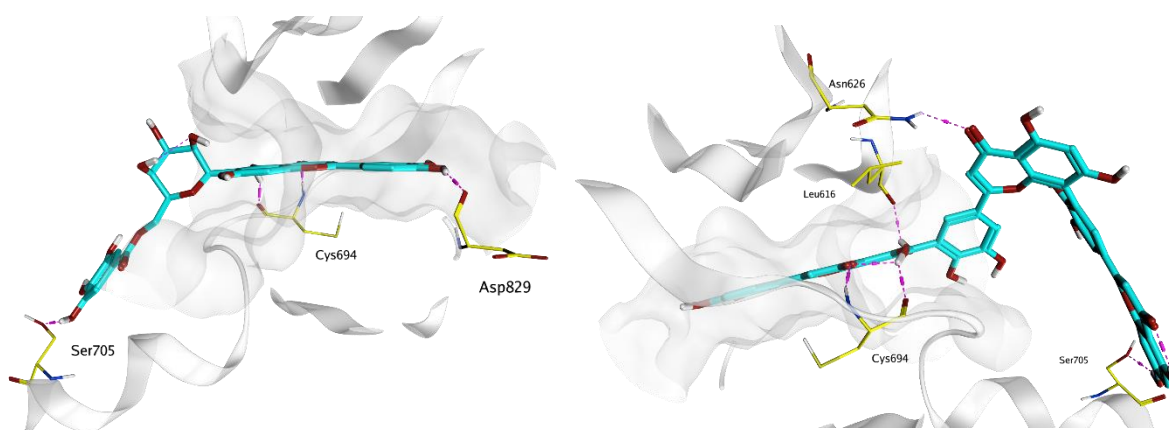


Figure 9: Interactions of compounds 7 and 8 inside the active site of the FLT3 kinase domain

Compound 9 with docking score (-15.966 kcal/mol) formed five H-bonds with residues Leu616 (1.980 Å—Acceptor and 1.740 Å—Acceptor), Glu661 (2.0 Å), Cys694 (1.950 Å), Arg834 (2.310 Å). Compound 10 with docking score (-15.772 kcal/mol) formed seven H-bond with residues Cys694 (1.70 Å), Ser705 (1.660 Å), Asp698 (1.960 Å), Asp829 (1.630 Å), Asn701 (2.190 Å), Glu661 (1.890 Å), Lys644 (1.740 Å).

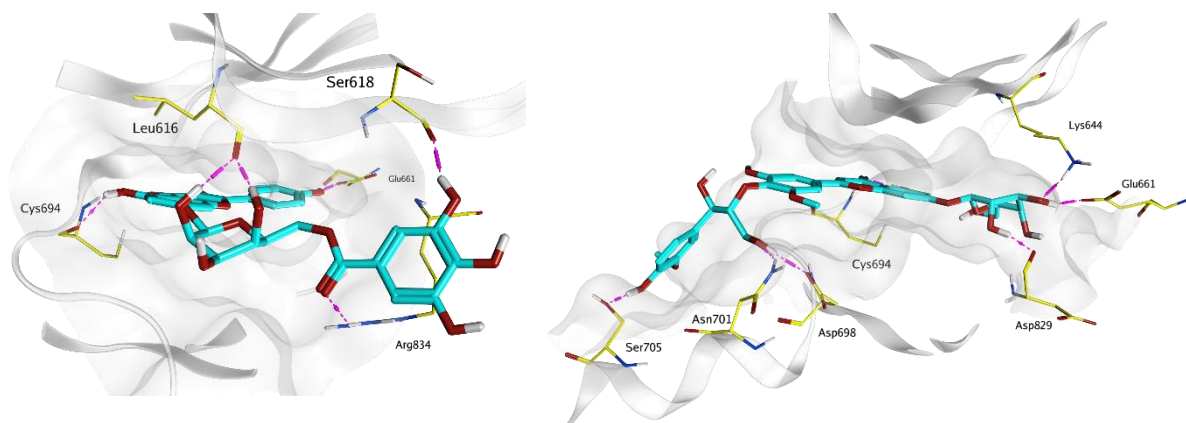


Figure 10: Interactions of compounds **9** and **10** inside the active site of the FLT3 kinase domain

Quizartinib, the co-crystal inhibitor of 4XUF with a docking score of -11.616 kcal/mol, formed two H-Bonds with residues Cys695 (2.080 Å) and Glu661 (2.040 Å); it was also used to validate the docking process by comparing the obtained pose with the crystal pose, which resulted in RMSD of 0.698 Å.

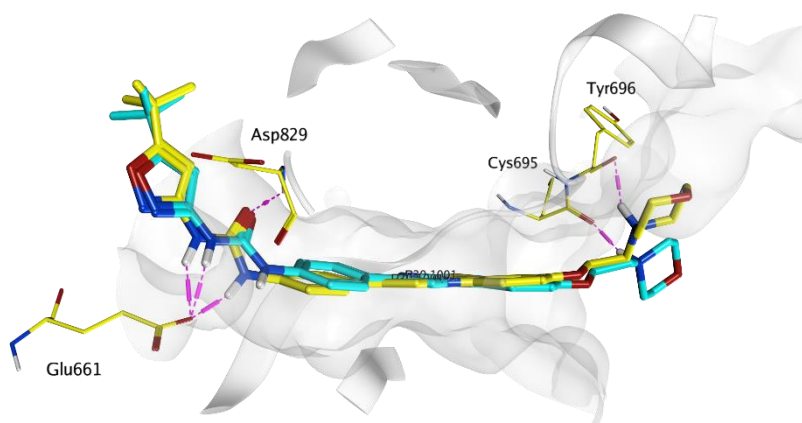


Figure 11: Interactions of the co-crystal inside the active site of the FLT3 kinase domain and overlay of the co-crystal pose (yellow) and docked pose (cyan)

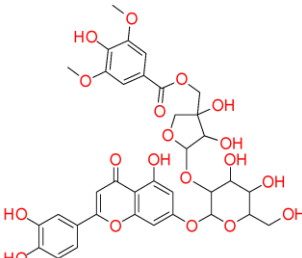
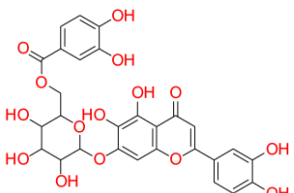
### Physiochemical properties

All compounds showed a molecular weight higher than 500 Da except compound 5, which had a molecular weight of 432.38 Da. Compounds 2, 4, 5, 7, 8, and 9 have less than ten rotatable bonds, while compounds 1, 3, 6, and 10 have less than fourteen rotatable bonds, which indicate that they will have a lower toxicity and higher selectivity index. [12]

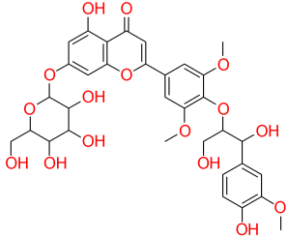
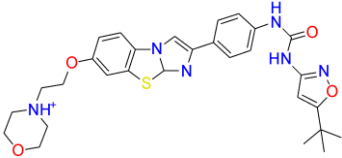
All compounds had over ten H-bond acceptors except for compound 5, which had ten H-bonds; notably, compound 1 had nineteen H-bond acceptors. Most compounds had H-bond donors within a range of eight to ten, while compounds 4 and 5 had 6 and 7 H-bond donors, respectively.

The topological surface area (TPSA), which counts for the number of oxygen and nitrogen atoms within the compound, TPSA is related to the brain blood barrier (BBB); the preferable TPAS is 70 -140 Å<sup>2</sup>, compounds with TPSA lower than 70 Å<sup>2</sup> will penetrate the BBB and will inter the CNS, which will lead to side effect issues, while compounds with TPSA higher than 140 Å<sup>2</sup> will have a short half-life time. All compounds have a topological polar surface area of more than 200(Å<sup>2</sup>), with compound 8 having the highest TPSA of 333.38 Å<sup>2</sup>. cLogP is a measure of compound lipophilicity; according to the rule of five, compound lipophilicity should not exceed five, and a clogP higher than five will cause the compound to have solubility and permeability issues [13]. Most compounds showed a clogP lower than 1.35. Finally, compounds 1, 2, 3, 6, 9, and 10 were moderately soluble, while compounds 4, 5, and 7 were soluble.

Table 2: Physicochemical properties

ID	Structure	MW	Rota-table Bonds	H-bond acceptors	H-bond donors	TPSA	Consensus Log P	ESOL Class
1		760.65	12	19	9	293.96	0.12	Moderately soluble
2		600.48	7	15	9	257.04	0.26	Moderately soluble

<b>3</b>		740.66	10	17	9	275.5	0.54	Moderately soluble
<b>4</b>		533.42	8	14	6	236.48	-0.56	Soluble
<b>5</b>		432.38	3	10	7	181.05	-0.12	Soluble
<b>6</b>		756.66	10	18	10	295.73	0.04	Moderately soluble
<b>7</b>		600.48	6	15	10	268.04	-0.03	Soluble
<b>8</b>		854.68	5	18	12	333.39	4.16	Poorly soluble
<b>9</b>		600.48	7	15	9	257.04	0.4	Moderately soluble

<b>10</b>		688.63	12	16	8	247.43	0.75	Moderately soluble
<b>Quizar tinib</b>		561.68	10	6	3	135.6	3.6	Poorly soluble

### Molecular dynamics

The docking procedure lacked the flexibility of the protein residue; hence, to validate the results obtained from the docking step, molecular dynamic (MD) simulations were implemented. MD mimics the cell environment, where the ligand-protein complex immerses in a box of water with Na and Cl as neutralizer ions, Figure 10.

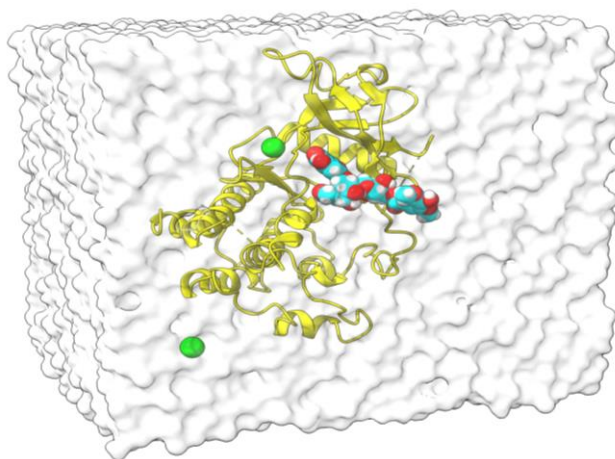


Figure 12: The ligand(cyan) – protein(yellow) complex surrounded by water (white box) and Cl atoms (green balls)

Compounds **1**, **2**, and **3**, along with the reference drug, were subject to 100 ns molecular dynamic simulations inside the active site of the FLT3 kinase domain.

The root mean square deviation (RMSD) was used to monitor the conformational of the protein backbone in addition to the movement of the ligand inside the active site, considering the first frame of the simulation as a reference.

## Protein RMSD

The conformation of the protein backbone during the MD simulation is critical; a protein that fluctuates higher than 3.00-4.00 Å considered unstable, and denaturation is taking place. [12]

The RMSD of the ligand-protein complexes is monitored during the simulation as a function of time, with respect to  $C\alpha$  initial position. [12] The obtained RMSD is plotted in Figure 11. As can be seen in Figure 11, most protein complexes were stable with RMSD of less than 2.5 Å, which indicates that these compounds do not affect the protein conformation during the simulation.

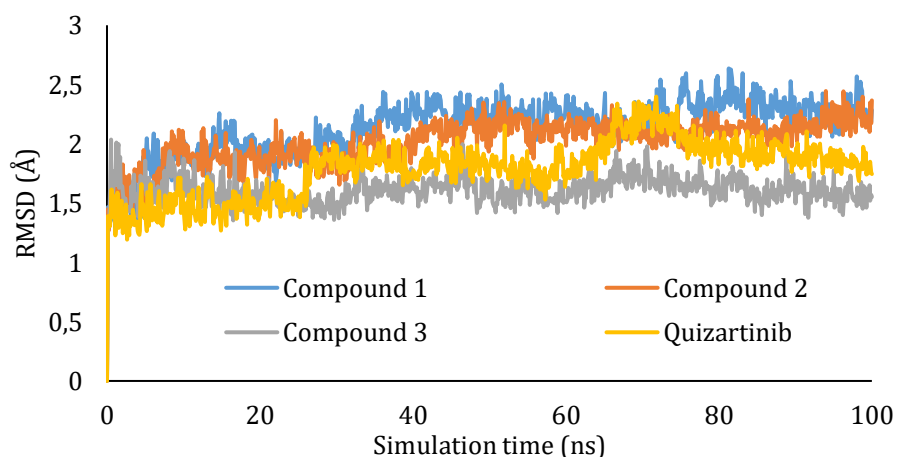


Figure 13: The RMSD of the  $C\alpha$  atoms of the protein backbone of compounds **1**, **2**, **3**, and quizartinib – protein complexes.

The ligands RMSD were also monitored during the simulation with respect to their initial position inside the active site of the protein and reported as a function of time, Figure 12.

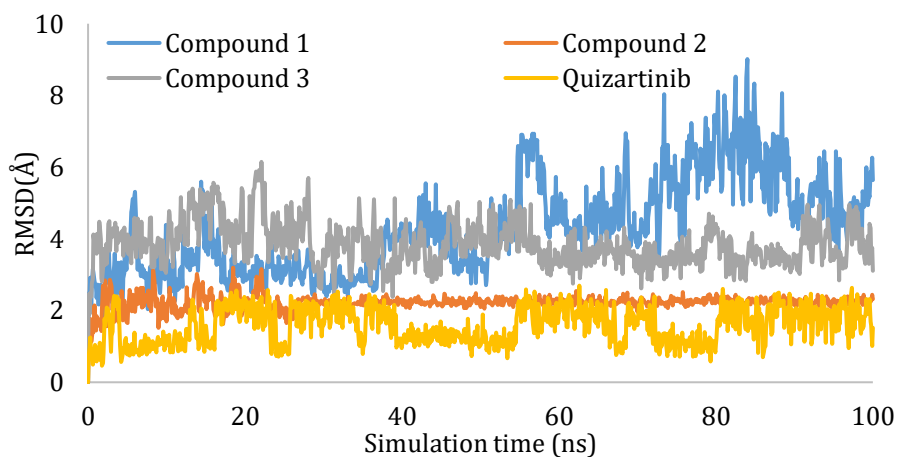


Figure 14: The RMSD of the heavy atoms of the compounds 1, 2, 3, and quizartinib – protein complexes.

As can be seen in Figure 12, compound **1** starts to fluctuate from the beginning till the end of the simulation and reaches an RMSD of 9.00 at around 80 ns of the simulation time; this fluctuation is coming from the movement of the ligand outside the active site of the protein as it can be seen in Figure 13.

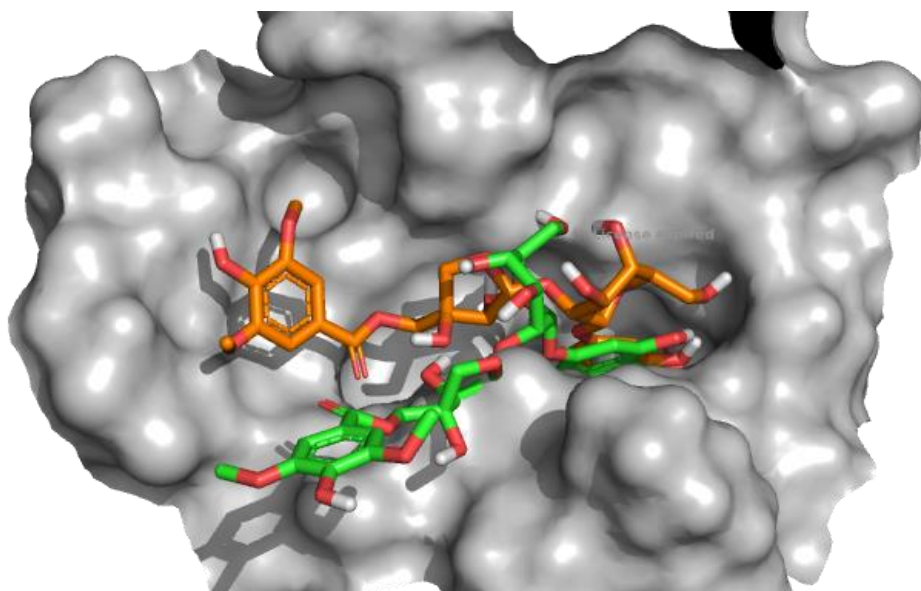


Figure 15: Snapshoots of compound **1** at 0ns (orang) and 100ns(green) of simulation time inside the active site of the protein



On the other hand, compound **2** was so stable inside the active site of the protein that it moved by 2.00 Å at the beginning of the simulation and held the position till the end of the simulation.

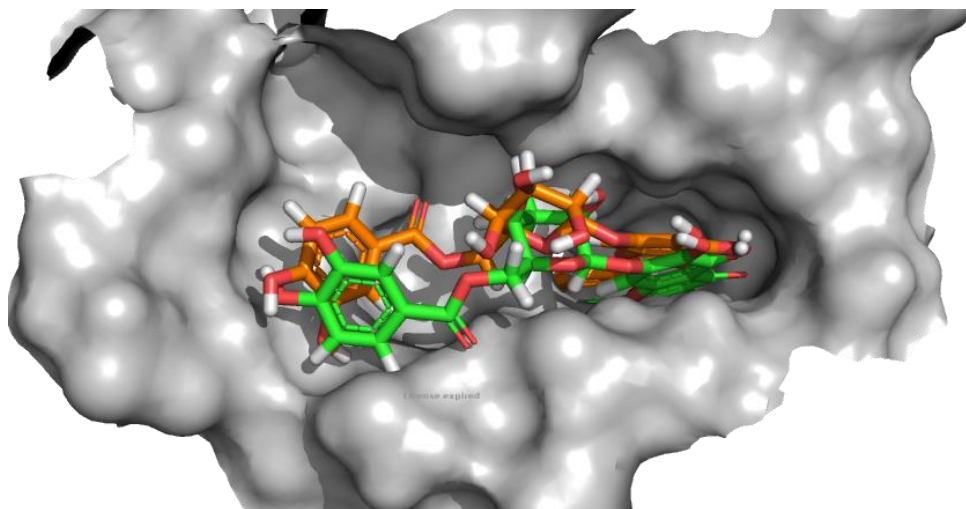


Figure 16: Snapshots of compound **2** at 0ns (orang) and 100ns(green) of simulation time inside the active site of the protein.

Compound **3** showed a fluctuation at around 4.00 Å from the start to the end of the simulation time. This fluctuation is due to the size of compound **3**, which makes it able to form and lose H-bonds with surrounding residues, Figure 15.

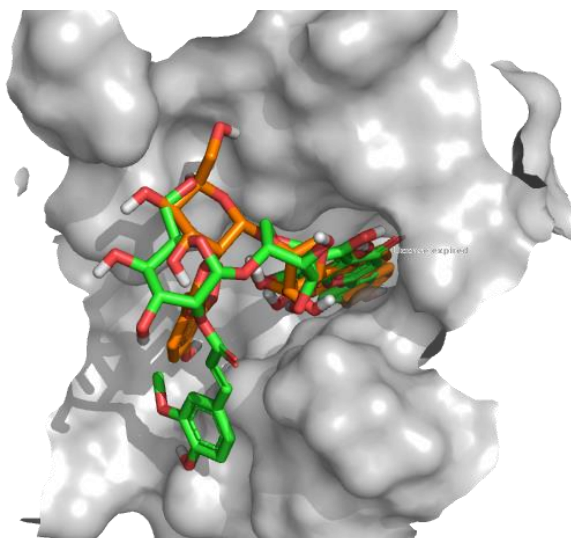


Figure 17: Snapshoots of compound **3** at 0ns (orang) and 100ns(green) of simulation time inside the active site of the protein



Finally, quizartinib showed good stability inside the active site of the protein, with an RMSD of less than 2.00 Å from the start till the end of the simulation, Figure 16.

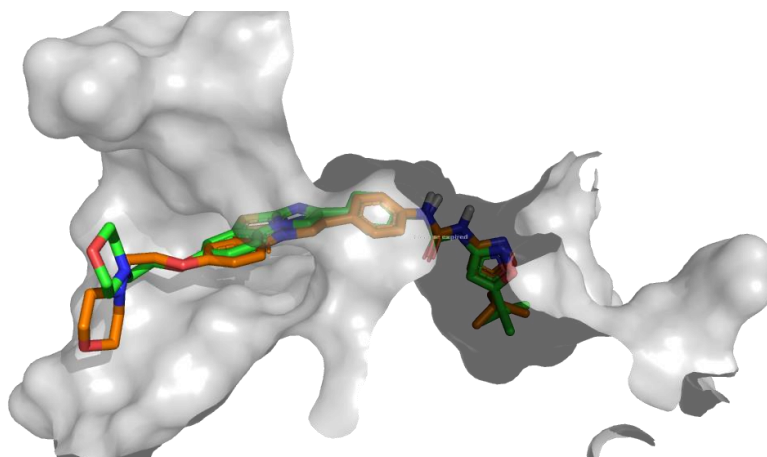


Figure 18: Snapshots of the quizartinib at 0ns (orang) and 100ns(green) of simulation time inside the active site of the protein

### Protein-Ligand Contacts

Next, a close look at the interaction between the three compounds and the protein residues was conducted, Figure 17. The result is reported as a percentage, where 100% represents interaction throughout the whole time, and a higher percentage than 100% indicates more than one interaction with the same residue. Compound **1** showed a solid H-bond interaction with residing Cys694, Asp829, Asp835, and Lys644 in addition to the water bridge H-bond toward Asp698. Compound 1 interacts via Van der Waal's (VdW) interaction with Ala626, Leu818, and Phe830. Compound 2 also was able to get a strong H-bond interaction with residue Asp698, Asp839, Cys694, and Asp829. Finally, compound **3** had a strong H-bond toward Cys694 only, with multiple VdW interactions and water bridge H-bonds.

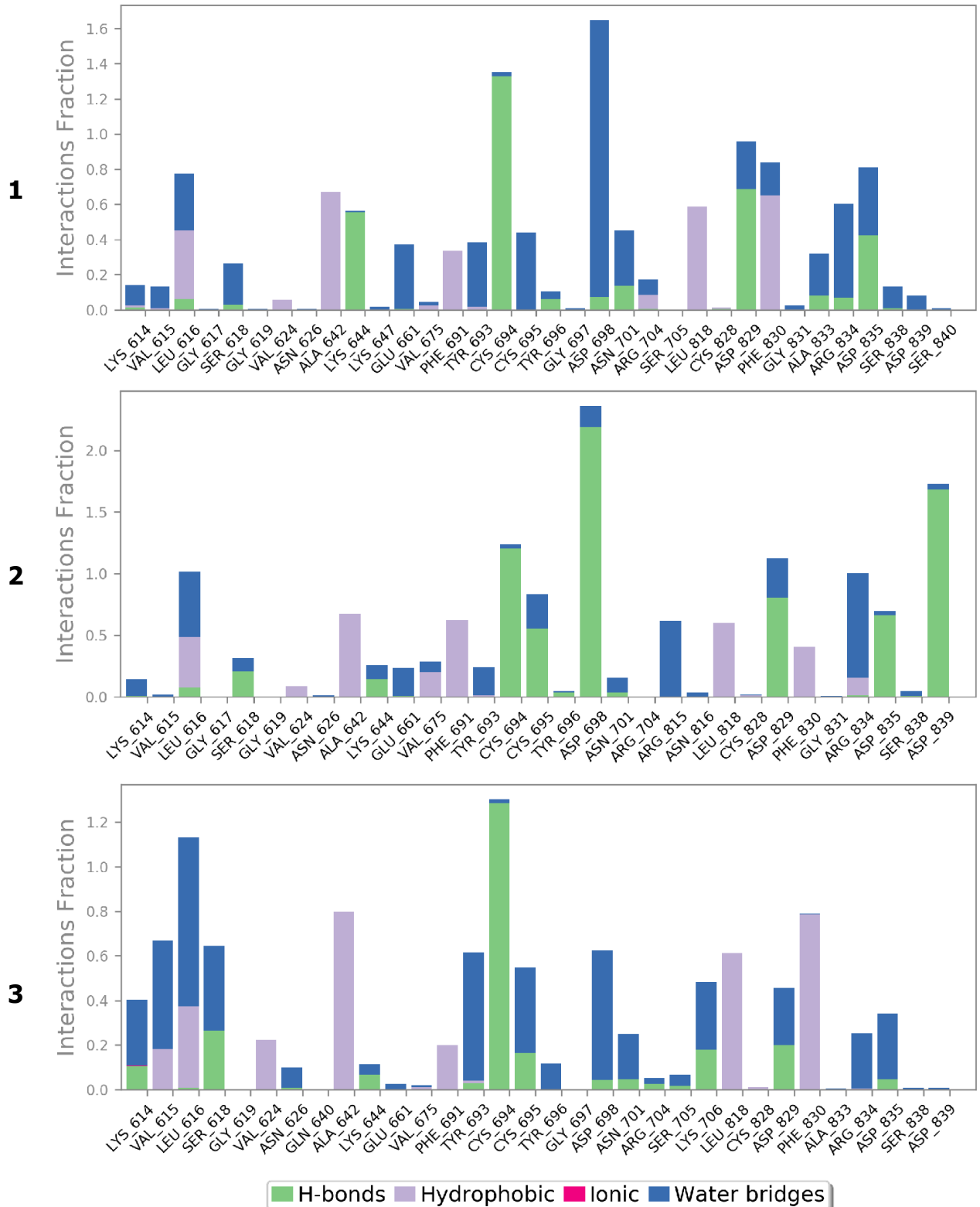


Figure 19: Protein-ligand contacts of compounds 1, 2, and 3 toward the active site residues of the FLT3 kinase domain

## **Material and methods**

All studies were conducted using Schrödinger software.

### Molecular Docking

The docking studies were conducted using the Maestro package of Schrödinger LLC, which is a powerful software platform for molecular modeling, simulations, and drug discovery; it provides tools for molecular design, virtual screening, visualization, and analysis [14]. First, the Collection of Open Natural Products (COCONUT) database, which contains 407,270 natural products, provides a wealth of information about natural products, including their chemical structures, biological activities, and sources, was downloaded from <https://coconut.naturalproducts.net>. The database was filtered, and compounds with molecular weight higher than 1000 g/mol were eliminated, along with compounds with a cLogP higher than 10, which resulted in a database of 192,560; the obtained database was washed (removing ions), protonated (adding hydrogens), and minimized (optimizing the bond length, angle, and dihedral), which made it ready to be docked. Next, the crystal structure of the FLT3 kinase domain was retrieved from the protein data bank (PDB ID: 4XUF, 3.20 Å) in complex with quizartinib as a co-crystal ligand. Finally, the protein was prepared (washed, protonated, and minimized) using the Quickprep panel and OPLS4 as a force field. Default settings were used for the docking procedure.[15]

### Molecular dynamics

The MD simulations were carried out using the Desmond simulation package of Schrödinger LLC, according to our previous publications' protocols. The NPT ensemble with a temperature of 300 K and a pressure of 1 bar was applied in all runs. The simulation length was 200 ns with a relaxation time of 1 ps. The OPLS3 force field parameters were used in all simulations. [16-22]

### Physicochemical properties

SwissADME was used to conduct additional pharmacokinetic studies, which offer comprehensive analysis related to drug properties and Absorption, Distribution, Metabolism, and Excretion parameters such as bioavailability, drug-likeness, and potential toxicity, in addition to giving indications about the suitability of a compound for further development. [23]

## **Conclusions**

In this study, we screened the COCONUT database of African Natural Products to identify potential inhibitors against the FLT3 kinase domain (PDB ID: 4XUF) to treat acute

myeloid leukemia. Out of the compounds screened, ten showed better docking scores compared to the reference drug Quizartinib (Docking Score -11.616kcal/mol). Compound 1 had a docking score of (-18.052 kcal/mol), while compound 2 had a docking score of (-17.884 kcal/mol). Both compounds formed H-bonds with the receptor residues and had desirable physicochemical properties, including moderate solubility and molecular weight of more than 500 Da.

Furthermore, these candidate compounds exhibited lower toxicity and more excellent selectivity to FLT3 receptors as they had an average number of rotatable bonds. Most of the compounds showed limited GI absorption, with no BBB penetration nor Cytochrome P450 isoenzyme interactions. Molecular dynamic simulations indicated that compound 2 remained stable within the active site throughout the simulation when compared with other compounds, suggesting its potential for further in vitro testing.

### Acknowledgements

The authors acknowledge the Centre for High Performance Computing (CHPC), South Africa, for providing computational resources to this research project.

### References

- [1] Gebru, M.; Wang, H.; Therapeutic targeting of FLT3 and associated drug resistance in acute myeloid leukemia. *J. Hematol Oncol.* **2020**, 13, 1–13. DOI: [10.1186/s13045-020-00992-1](https://doi.org/10.1186/s13045-020-00992-1)
- [2] Barley, K.; Navada, S.; Acute myeloid leukemia. *J. Oncology.* **2019**, 308–318, DOI [10.1002/9781119189596.ch27](https://doi.org/10.1002/9781119189596.ch27)
- [3] Mohan, H.; Textbook of Pathology, 7<sup>th</sup> ed. **2015**, The Health Sciences Publishers.
- [4] Orgueira, A.; Pérez, L.; Torre, A.; Raíndo, A.; López, M.; Arias, J.; Ferro, R.; Rodríguez, B.; Pérez, M.; Ferreiro, M.; Vence, N.; Encinas, M.; López, J.; Martinelli, G.; Cerchione, C.; FLT3 inhibitors in the treatment of acute myeloid leukemia: current status and future perspectives. *J. Minerva Med.* **2020**, 111, 5. DOI: [10.23736/S0026-4806.20.06989-X](https://doi.org/10.23736/S0026-4806.20.06989-X)
- [5] Daver, N.; Schlenk, R.; Russell, N.; Levis, M.; Targeting FLT3 mutations in AML: review of current knowledge and evidence. *J. Leukemia.* **2019**, 33, 299–312. DOI: [10.1038/s41375-018-0357-9](https://doi.org/10.1038/s41375-018-0357-9)
- [6] Yamaura, T.; Nakatani, T.; Uda, K.; Ogura, H.; Shin, W.; Kurokawa, N.; Saito, K.; Fujikawa, N.; Date, T.; Takasaki, M.; Terada, D.; Hirai, A.; Akashi, A.; Chen, F.; Adachi, Y.; Ishikawa, Y.; Hayakawa, F.; Hagiwara, S.; Naoe, T.; Kiyoi, H.; A novel irreversible FLT3 inhibitor, FF-10101, shows excellent efficacy against AML cells with FLT3 mutations. *J.*

- Blood*. **2018**, 131, 426–438. DOI: [10.1182/blood-2017-05-786657](https://doi.org/10.1182/blood-2017-05-786657)
- [7] Kiyoi, H.; Kawashima, N.; Ishikawa, Y.; FLT3 mutations in acute myeloid leukemia: Therapeutic paradigm beyond inhibitor development. *J. Cancer Sci.* **2020**, 111, 312–322. DOI: [10.1111/cas.14274](https://doi.org/10.1111/cas.14274)
- [8] Wang, Z.; Jiongheng, C.; Jie, C.; Wenqianzi, Y.; Yifan, Z.; Hongmei, L.; Tao, L.; Yadong, C.; Shuai, L.; FLT3 Inhibitors in Acute Myeloid Leukemia: Challenges and Recent Developments in Overcoming Resistance. *J. Med. Chem.* **2021**, 64, 2878–2900. <https://doi.org/10.1021/acs.jmedchem.0c01851>
- [9] Tong, L.; Xuemei, L.; Yongzhou, H.; Tao, L.; Recent advances in FLT3 inhibitors for acute myeloid leukemia, *J. Future Med. Chem.* **2020**, 12, 961–981. <https://doi.org/10.4155/fmc-2019-0365>
- [10] Huang, M.; Lu, J.; Ding, J.; Natural Products in Cancer Therapy: Past, Present and Future, *J. Nat. Products Bioprospect.* **2021**, 11, 5–13. DOI: [10.1007/s13659-020-00293-7](https://doi.org/10.1007/s13659-020-00293-7)
- [11] Herschlag, D.; Pinney, M.; Hydrogen Bonds: Simple after All?. *J. Biochemistry.* **2018**, 57, 3338–3352. <https://doi.org/10.1021/acs.biochem.8b00217>
- [12] Alnajjar, R.; Mohamed, N.; Kawafi, N.; Bicyclo[1.1.1]Pentane as Phenyl Substituent in Atorvastatin Drug to improve Physicochemical Properties: Drug-likeness, DFT, Pharmacokinetics, Docking, and Molecular Dynamic Simulation. *J. Mol. Struct.* **2021**, 1230. <https://doi.org/10.1016/j.molstruc.2020.129628>
- [13] Lipinski, C.; Lead- and drug-like compounds: The rule-of-five revolution. *J. Drug Discovery Today: Technologies.* **2004**, 1, 337–341. <https://doi.org/10.1016/j.ddtec.2004.11.007>
- [14] Maestro, Schrödinger. "Maestro." Schrödinger, LLC, New York, NY, **2020**.
- [15] Farouk, F.; Elmaaty, A.; Elkamhawy, A.; Tawfik, H.; Alnajjar, R.; Abourehab, M.; Al-Karmalawy, A.; Investigating the potential anticancer activities of antibiotics as topoisomerase II inhibitors and DNA intercalators: in vitro, molecular docking, molecular dynamics, and SAR studies. *J. Enzyme Inhibit. Med. Chem.* **2023**, 38, 217-1029. DOI: [10.1080/14756366.2023.2171029](https://doi.org/10.1080/14756366.2023.2171029)
- [16] Release, S.; 3: Desmond molecular dynamics system, DE Shaw research, New York, NY, **2017**, Maestro-Desmond Interoperability Tools, Schrödinger, New York, NY **2017**.
- [17] Harder, E.; Damm, W.; Maple, J.; Wu, C.; Reboul, M.; Xiang, J.; Wang, L.; Lupyan, D.; Dahlgren, M.; Knight, J.; Kaus, J.; Cerutti, D.; Krilov, G.; Jorgensen, W.; Abel, R.; Friesner, R.; OPLS3: A Force Field Providing Broad Coverage of Drug-like Small Molecules and Proteins. *J. Chem. Theor. Comput.* **2016**, 12, 281-296. DOI: [10.1021/acs.jctc.5b00864](https://doi.org/10.1021/acs.jctc.5b00864)
- [18] Jorgensen, W.; Chandrasekhar, J.; Madura, J.; Impey, R.; Klein, M.; Comparison of simple

- potential functions for simulating liquid water. *J. Chem. Phys.* **1983**, 79, 926-935. <https://doi.org/10.1063/1.445869>
- [19] Neria, E.; Fischer, S.; Karplus, M.; Simulation of activation free energies in molecular systems. *J. Chem. Phys.* **1996**, 105, 1902-1921. <https://doi.org/10.1063/1.472061>
- [20] Release, S.; 4. Desmond Molecular Dynamics System, DE Shaw Research. Maestro-Desmond Interoperability Tools **2016**.
- [21] Martyna, G.; Klein, M.; Tuckerman, M.; Nosé–Hoover chains: The canonical ensemble via continuous dynamics. *J. Chem. Phys.* **1992**, 97, 2635-2643. DOI: [10.1063/1.463940](https://doi.org/10.1063/1.463940)
- [22] Martyna, G.; Tobias, D.; Klein, M.; Constant pressure molecular dynamics algorithms. *J. Chem. Phys.* **1994**, 101, 4177-4189. <https://doi.org/10.1063/1.467468>
- [23] Daina, A.; Michielin, O.; Zoete, V.; SwissADME: A free web tool to evaluate pharmacokinetics, drug-likeness and medicinal chemistry friendliness of small molecules. *J. Sci. Rep.* **2017**, 7. <https://doi.org/10.1038/srep42717>

**Copyright:** © 2023 by the authors. Submitted for possible open access publication under the terms and conditions of the Creative Commons Attribution (CC BY) license (<https://creativecommons.org/licenses/by/4.0/>).

